Pergamon

Bioorganic & Medicinal Chemistry, Vol. 4, No. 10, pp 1783–1794, 1996

PII: S0968-0896(96)00193-9
0968-0896/96 $15.00+0.00

Conformational Analysis of Phthalein Derivatives Acting as Thymidylate Synthase Inhibitors by Means of ^{1}H NMR and Quantum Chemical Calculations

Stefano Ghelli,[a,*] Giulio Rastelli,[b] Daniela Barlocco,[c] Marcella Rinaldi,[b] Donatella Tondi,[b] Piergiorgio Pecorari[b] and Maria Paola Costi[b,*]

[a]*Dipartimento di Chimica, Universita' di Modena, Via Campi 183, 41100 Modena, Italy*
[b]*Dipartimento di Scienze Farmaceutiche, Universita' di Modena, Via Campi 183, 41100 Modena, Italy*
[c]*Istituto Chimico Farmaceutico, Università di Milano, Viale Abruzzi 42, 20143, Italy*

Abstract—The conformations of a set of phthalein derivatives with bacterial thymidylate synthase (TS) inibitory activity were investigated by ^{1}H NMR spectra, performed at both room and low temperature, and by quantum chemical calculations. Since the crystal structure of the binary complex of phenolphthalein with the enzyme is known, we set out to study the conformation of various of its analogues in solution in order to observe the effects of the substituents on the phenolic rings, of the α-naphthol derivative and of the rigid analogue, fluorescein, and compare the results with the X-ray crystal structure studies. A relationship between the chemical shift of the proton on C4 (H4) of the phthalidic ring and the averaged angle formed by the phthalidic and the aromatic ring planes was found in which the most perpendicular conformations have the lowest H4 chemical shift values. At room temperature, the rotational freedom of all the studied compounds was similar, while at lower temperature the naphthol derivative assumed a partially blocked conformation. Finally, a qualitative relationship between the inhibitory properties of the compounds and their conformations is discussed. Copyright © 1996 Elsevier Science Ltd

Introduction

Thymidylate synthase (TS, EC 2.1.1.45) is an important target in the anticancer chemotherapy; inhibition of TS blocks the de novo synthesis of dTMP (thymidine-5′-monophosphate) starting from 2′-deoxyuridine-5′-monophosphate (dUMP), so that the synthesis of DNA cannot be accomplished and the cells die.[1] TS is a two substrates enzyme that catalyses the methylation of dUMP to dTMP; the catalytic reaction is assisted by the folate cofactor N5, N10-methylene-tetrahydrofolate that is the methyl donor.[2] The inhibition of TS can be obtained both by dUMP analogues and folate analogues, which act as antimetabolites.

Recently, it has been shown that some phthalein derivatives with non-analogue antifolate structures are good inhibitors of *Lactobacillus casei* TS (LcTS), our model enzyme, with a competitive inhibition pattern with respect to the folate cofactor.[3–5]

In the phthalein series, the more active compounds have the general structure of phenolphthalein: a planar phthalidic (isobenzofuranone) ring with a quaternary carbon unit, bearing two aromatic rings variously substituted (Fig. 1).

Keywords: conformational analysis, phthalein derivatives, thymidylate synthase, enzyme inhibition, ^{1}H NMR, quantum chemical calculations.

The X-ray crystal structure of phenolphthalein in the binary complex with *Lactobacillus casei* TS has been solved at 2.3 Å resolution.[3] The planes of the two phenolic rings assume different orientations with respect to the phthalidic ring (Fig. 2) and only a few hydrogen bonds with the binding site cavity are detected. Phenolphthalein binds in a position similar to that of dUMP, where the protein forms a cavity large enough to allow this compound a substantial conformational freedom. Therefore, it is possible that phenolphthalein binds TS, retaining its lower energy conformation. However, the hydrogen bonds with Asp 221 and Glu60 could impose restrictions on the orientation of these rings.

Therefore, it was interesting to investigate if the conformation of phenolphthalein observed in the enzyme binary complex is close to that observed in the unbound state; if the calculated and experimental observed conformations agree and if there is a relationship between the conformational properties of the inhibitors and their inhibitory activity against TS in order to understand if this aspect is relevant to the interpretation of the biological results.

With this aim, the conformations of the *o*-substituted phthalidic derivatives (**1–5**), of the α-naphthol derivative (**6**) and of fluorescein (**7**) were investigated by means of mono- and bi-dimensional ^{1}H NMR spectra, performed at both room and low temperature, and also by means of quantum chemical calculations. Moreover,

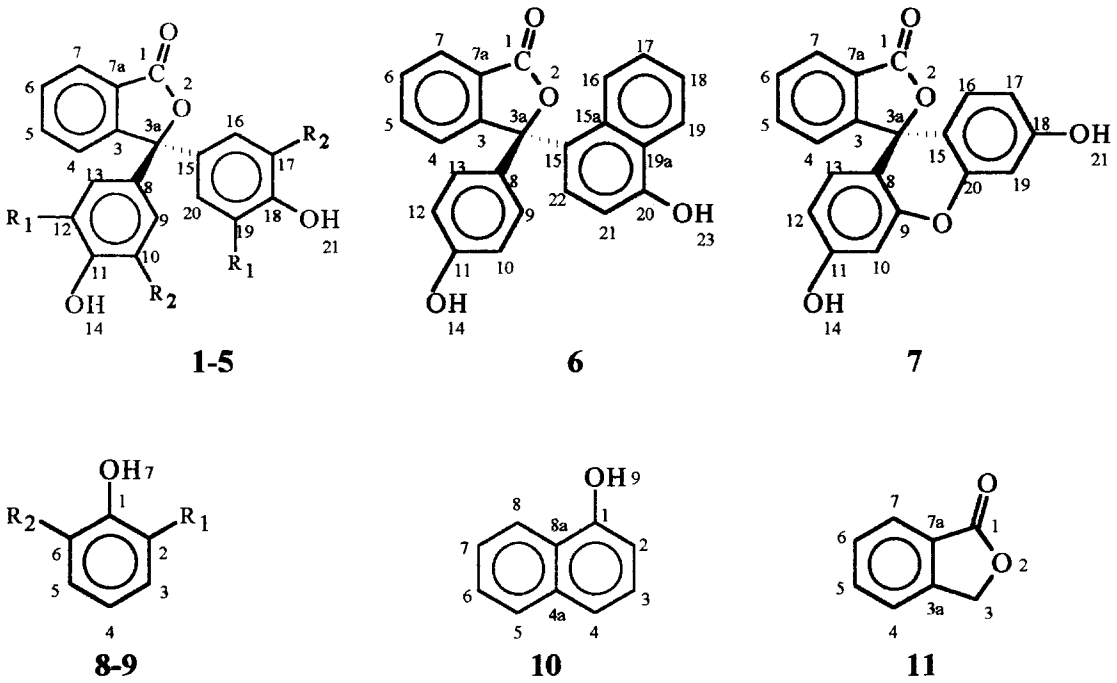

Figure 1. 1: $R_1 = R_2 = H$; 2: $R_1 = Cl$, $R_2 = H$; 3: $R_1 = R_2 = Cl$; 4: $R_1 = R_2 = Br$; 5: $R_1 = R_2 = I$; 8: $R_1 = R_2 = H$; 9: $R_1 = Cl$, $R_2 = H$.

we compared the results with those of the TS-binding ligands in the crystal structure.

Compounds **8–11** were studied in the same way as references for ^1H NMR studies; to complete the series, some compounds (**2**, **3**, and **5**) were synthesized and tested as inhibitors of LcTS.

Results and Discussion

^1H NMR spectroscopy

Characterization of the structures 1–7. One-dimensional proton NMR spectra of structures **1–7** show second-order scalar coupling effects and in some cases partial superimposition of the signals. For these reasons the peaks were assigned on the basis of the homocorrelation spectra (2-D COSY or selective 1-D COSY spectra) and the observed NOE in 2-D NOESY spectra. Table 1 reports the chemical shift, the spin multiplicities, the coupling constants (directly determined from the spectra without theoretical simulation), the most important correlations observed in the COSY spectra, and all observed NOEs in NOESY spectra of compounds **1–7**.

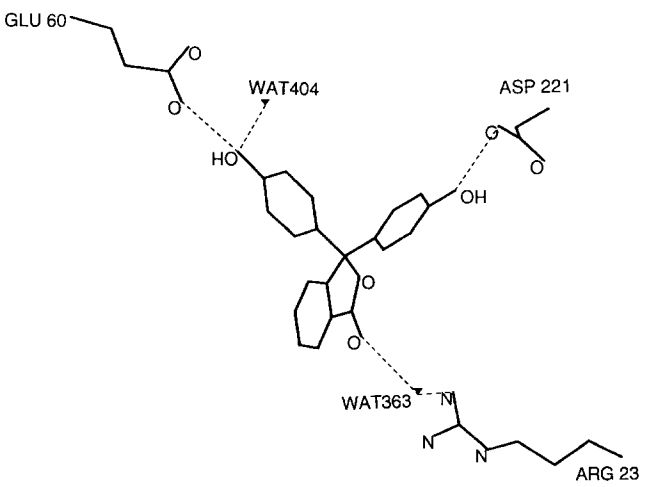

Figure 2. X-ray crystal structure of phenolphthalein in the binary complex with *Lactobacillus casei* TS at 2.3 Å resolution (3).

In the case of compounds **1–7**, NOEs were detected both at 200 ms and 600 ms of mixing time and all the molecules proved in negative NOE regime. The cross-peak intensities were larger in the second case. Spectra of compounds **1**, and **3–7** showed only two-spin system NOEs; therefore, we were confident to exclude spin-diffusion. The spectrum of compound **2** showed NOE between H4 and H9, H13 and between H4 and H10, H12. In this case, we cannot exclude spin diffusion; however, this does not change the correct assignement of proton H4, that was the starting point for the assignement of phthalidic protons through scalar correlations.

Conformational analysis from NMR. The data reported in Table 1 and plotted in Figure 3 show that the chemical shifts of H4 increase in the order **7**, **6**, **1**, **2**, **5**, **3**, and **4** by about 0.82 ppm (from 7.365 to 8.184 ppm); much lower effect is observed for H5 ($\Delta\delta = 0.201$ ppm). The chemical shifts of H6 ($\Delta\delta = 0.27$ ppm) and H7 ($\Delta\delta = 0.192$ ppm) also changes slightly in the series **1–7** but show a different trend with respect to the former protons.

This behaviour is due to the different intensity of the current ring effect induced by the aromatic ring on the

Table 1. NMR data for compounds **1–6**

H	Compound **1**		Compound **2**		Compound **3**	
	δ (ppm)	*J* (Hz)	δ (ppm)	*J* (Hz)	δ (ppm)	*J* (Hz)
H4	7.839 ddd	7.7; 0.8; 0.9	7.990 ddd	7.8; 1.4; 0.8	8.18 dd	7.6; 0.8
H5	7.911 ddd	7.7; 7.2; 1.0	7.955 td	7.8; 1.1	7.998 tt	7.6; 0.8
H6	7.737 ddd	7.6; 7.2; 0.9	7.780 ddd	7.8; 7.6; 1.4	7.802 tt	7.6; 0.8
H7	7.988 ddd	7.6; 1.0 ; 0.8	8.020 ddd	7.6; 1.1; 0.8	8.037 dd	7.6; 0.8
H9, H16	7.163 ddd	8.8; 3.9; 2.2	7.185 dd	8.5; 2.3	7.380 s	—
H10, H17	6.842 ddd	8.8; 3.0; 2.2	7.078 d	8.5	—	—
H12, H19	≡ H10	≡ H10	—	—	—	—
H13, H20	≡ H9	≡ H9	7.265 d	2.3	≡ H9	≡ H9
H14, H21	9.727 s	—	10.620 s	—	10.680 s	—

H	Compound **4**		Compound **5**		Compound **7**	
	δ (ppm)	*J* (Hz)	δ (ppm)	*J* (Hz)	δ (ppm)	*J* (Hz)
H4	8.184 ddd	7.5; 0.9; 0.8	8.116 ddd	7.5; 0.9; 0.8	7.365 d	7.6
H5	8.002 td	7.5; 0.8	7.993 td	7.5; 0.8	7.811 t	7.6
H6	7.812 ddd	7.8; 7.5; 0.9	7.803 td	7.5; 0.9	7.890 t	7.6
H7	8.043 dt	7.8; 0.8	8.035 dt	7.5; 0.8	8.08 d	7.6
H9, H16	7.528 s	—	7.681 s	—	—	—
H10, H17	—	—	—	—	6.030 d	1.86
H12, H19	—	—	—	—	6.104 dd	9.28, 1.86
H13, H20	≡ H9	≡ H9	≡ H9	≡ H9	6.641 d	9.07
H14, H21	10.450s	—	9.980 s	—	10.210 s	—

H	Compound **6**		Compound **6**[a]		Compound **6**[b]	
	δ (ppm)	*J* (Hz)	δ (ppm)	*J* (Hz)	δ (ppm)	*J* (Hz)
H4	7.701 d	7.6	7.790d	7.7	7.810 d	7.7
H5	7.931 td	7.6; 1.2	8.001 t	7.7	8.040 t	7.7
H6	7.758 td	7.6; 0.8	7.850 t	7.5	7.870 t	7.4
H7	8.046 d	7.6	8.120 t	overlapped	8.170 t	7.4
H9	7.058 dt	8.7; 3.1; 2.0	7.215 d	8.3	7.040 d	broad
H10	6.773 dt	8.7; 3.1; 2.0	6.920 d	8.3	6.810 d	broad
H12	≡ H10	≡ H10	≡ H10	≡ H10	6.940	broad
H13	≡ H9	≡ H9	≡ H9	≡ H9	7.530	broad
H14	9.615 s	—	9.106 s	—	9.680 s	—
H16	7.950 d	8.5	8.120 t	overlapped	8.090 t	8.6
H17	7.441 ddd	8.5; 6.8; 1.4	7.520 t	7.7	7.560 t	7.7
H18	7.518 ddd	8.5; 6.8; 1.4	7.613 t	6.7	7.650 t	6.7
H19	8.295 dd	8.5; 1.0	8.444 d	8.0	8.430 d	8.0
H21	6.877 d	8.2	6.958 d	8.0	6.970 d	7.7
H22	7.297 d	8.2	7.408 d	8.0	7.380 d	7.7
H23	10.609 s	—	10.081 s	—	10.710 s	—

Compound	Correlations
1	C:H7-H6; H6-H5; H5-H4; - **N**:H4-(H9, H13, H16, H20)
2	SC:H7-H6; - **N**: H4-(H9, H20); H4-(H13, H16); H14-(H10, H12)
3	SC:H7-H6; H5-H4; - **N**:H4-(H9, H13; H16, H20)
4	SC:H7-H6; H5-H4; - **N**:H4-(H9, H13; H16, H20)
5	SC:H7-H6; H5-H4; - **N**:H4-(H9, H13; H16, H20)
6	C:H7-H6; H7-H5; H7-H4; H6-H5; H6-H4; H5-H4; (H9,H12)-(H10,H11); H22-H21; H19-H18; H19-H17; H19-16; H18-H17; H18-H16; H17-H16; - **N**:H4-(H9, H13); H4-H22; H4-H16; H16-(H9, H13); (H9,H13)-H22(s); H14-(H10, H12); H23-H21; H23-H19
6[a]	N:H4-H21; H4-H22; H5-H22; H9-H10; H12-H13; H14-H10; H14-H9; H23-H21; H23-H19(s)

Proton chemical shift (δ), spin multiplicities (s, singlet; d, doublet; t, triplet), coupling constants and main scalar and dipolar correlations (C, correlation in 2-D COSY spectra; SC, correlation in 1-D selective-COSY spectra; N, correlation in 2-D NOESY spectra (Hn–Hm means correlation between proton Hn and proton Hm; s means small effect)) of compounds **1–7** dissolved in DMSO-d_6 at room temperature. **6**[a] and **6**[b] are referred to compound **6** disssolved in acetone-d_6 at room temperature and at 179 K, respectively. All chemical shifts are referred to residual signal of DMSO-d_6 positioned at 2.6 ppm.

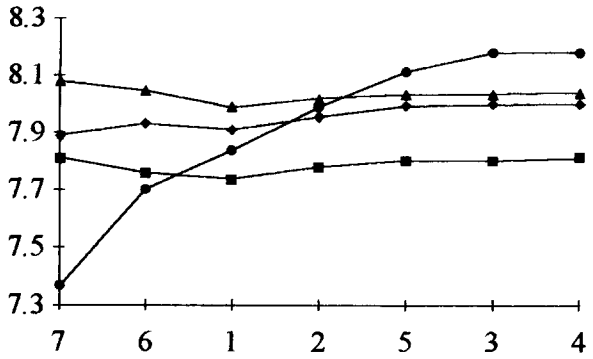

Figure 3. ^{1}H chemical shifts of H4 (●), H5 (▲), H6 (■), and H7 (◆) protons of the phthalidic ring in series **1–7**.

phthalidic protons that depends on two factors: (a) the position of the protons on the phthalidic ring, proton H4 thus being more sensitive than all the other phthalidic protons because it is closest to the phenolic ring; and (b) the angle formed in each case by the phthalidic ring and the planes of the aromatic rings. When the angle is close to perpendicularity, the shielding cones of the phenolic rings are oriented towards the phthalidic ring (structure **7**). Conversely, the more the angles deviate from 90°, the less the protons of the phthalidic ring fall inside the shielding cones of the phenolic ring. The chemical shift of proton H4 shows that the angles of the phenolic rings should decrease as follows: **7**, **6**, **1**, **2**, **5**, **3**, **4** (Fig. 3). On the other hand, the differences in the chemical shifts of protons H5, H6, and H7 are difficult to rationalize since they are too small and can be affected by additive effects such as the presence of the carbonyl group. Only variations in the chemical shift of H4 are therefore taken into account for purposes of conformational analysis.

Moreover, comparing the proton chemical shifts of aromatic rings bound to C-3 in structures **1–7** (Table 1) with those of the corresponding free rings, structures **8–11** (Table 2), it can be observed that the free molecules and the linked fragments have very similar chemical shifts. This suggests a substantial rotational freedom of the two aromatic fragments around the C3—C8 and C3—C15 bonds. In fact, if preferred conformations exist, the ring current effects should be of higher intensity, especially for conformations in which the two aromatic rings are perpendicular to each other. This is confirmed by NOE data as well. NOEs of around 2% have been observed in structures **1–5** between H4 and protons H9, H13, H16, and H20. Moreover, in compound **2**, the only structure in which signals of H9 and H16 can be distinguished from those of H13 and H20, NOE H4–H9, H16 and H4–H13, H20 have almost the same intensities. In compound **6**, NOE H4–H9, H13, H4–H16, and H4–H22 have a similar intensity, while a very weak effect between H9–H13 and H9–H22 was also observed. These data are indicative of rotational freedom around C3–C8 and C3–C15 bonds that are not reduced by steric hindrance owing to the presence of *ortho* substituent on phenolic rings. Only the presence of α-naphthol ring in compound **6** seems to induce a slight preference for conformations in which H22 is orientated towards the phthalidic ring rather than towards the phenolic ring.

With a view to comparing the conformations of the molecules in the crystal structure of the binary complex with LcTS and those predicted by quantum chemical calculations with the conformations in solution, we studied the boundary structures, in the series **1–7**, at different temperatures from room temperature to 179 K. At low temperature, the NMR derived structure is closer to that in crystal state and, as shown in the next section, to that calculated by quantum chemical analysis, so the experimental and theoretical results are more easily compared. Compound **1** did not show any change in its ^{1}H NMR spectrum with the decrease in temperature: this means that the structure has substantial rotational freedom around the C3–C8 and C3–C15 bonds even at low temperature.

On the other hand, compound **6** exhibited marked enlargement of the signals H9 and H13, starting at 240 K, and H10 and H12 starting at 220 K (Fig. 4). With the decrease in temperature, the former signal becomes larger and larger until at 179 K it gives rise to two new well-separated signals: one highfield shifted by about 0.275 ppm, the other downfield shifted by about 0.315 ppm (Table 1). Similarly, the signal of protons H10 and H12 at 179 K gives rise to two new well separated signals: one highfield, shifted by about 0.1 ppm, and one downfield, shifted by about 0.12 ppm.

Assignments of these peaks were enabled by the 2-D NOESY spectrum at 179 K in which the signals of H10 and H12 can be distinguished from those of H9 and H13, because both H10 and H12 show a strong NOE with the oxydrilic proton, H14.

Moreover, a weak NOE between H4 and H13 or H9 is observable. We decided to assign this NOE to interation with H13; hence, H9, H10, and H12 were assigned.

The 2-D NOESY spectrum also shows the following NOE: H4–H22, H4–H21, H5–H22 (weak), and H9-H16 (weak); whereas no NOE is found between H4 and H16 (Fig. 5).

Chemical shifts of protons H9, H10, H12, and H13 support the view that, at low temperature, a well-defined conformation of phenolic ring is present and the observed NOEs confirm this hypothesis. Moreover, NOEs led us to conclude that protons H21 and H22 pointing towards the phthalidic ring (see the presence of NOE H4–H22, H4–H21, and the absence of NOE H4–H16) and the phenolic ring is orientated towards the plane of the phthalidic ring so that only H13 is pointing towards H4 (no NOE had been observed between H4 and H9), while H9 is on the opposite side as confirmed by NOE H9–H16 (see Fig. 8 in the Conclusion).

NOE between H4 and H22 could be due to cross-relaxation between H22 and H21. Similarly, NOE between

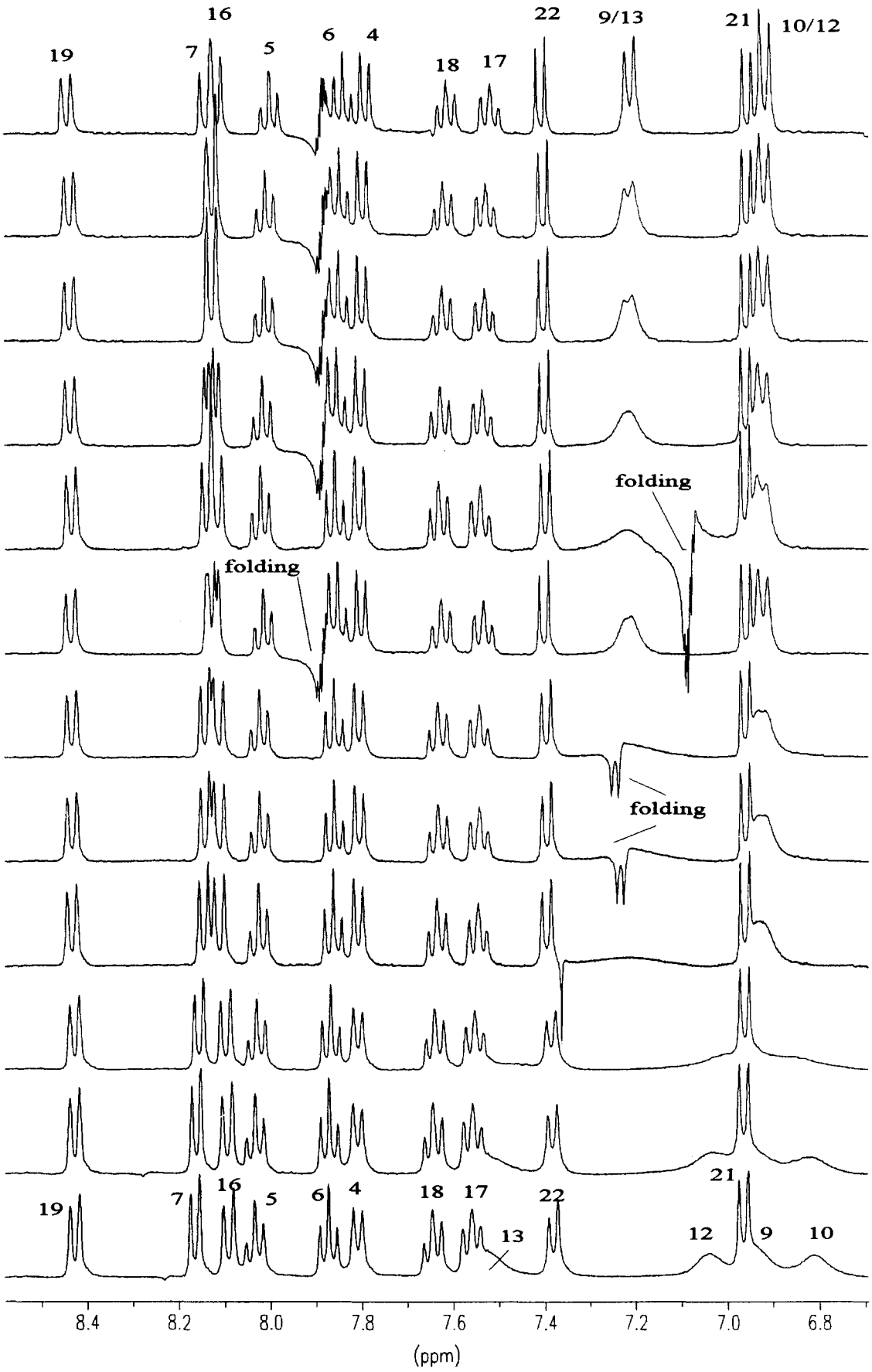

Figure 4. ^{1}H NMR spectra of compound **6** at different temperatures.

Table 2. Chemical shifts (δ) and difference of chemical shifts (Δδ) of compounds **8–11**

H	**8** δ (ppm)	**9** δ (ppm)	**10** δ (ppm)	**11** δ (ppm)	**8→1** Δδ (ppm)	**8→6** Δδ (ppm)	**9→2** Δδ (ppm)	**10→6** Δδ (ppm)
H2	≈ 6.844	—	6.960	—	+0.002	+0.071	—	+0.083
H3	7.250	7.095	7.400	5.523	+0.087	+0.192	+0.017	+0.103
H4	≈ 6.854	7.218	7.430	7.9577	—	—	+0.033	—
H5	≡H3	6.872	7.905	7.6964	≡H3	≡H3	—	−0.045
H6	≡H2	7.400	7.556	7.8866	≡H2	≡H2	+0.135	+0.115
H7	—	—	7.529	7.7855	—	—	—	+0.011
H8	—	—	8.220	—	—	—	—	−0.075
OH-	9.407	10.185	10.165	—	−0.320	−0.208	−0.43	−0.444

H5 and H22 could be due to cross-relaxation between H4 and H5. However, spin diffusion would not change the above discussion because protons H4 and H5 and protons H22 and H21 are on the same side of the molecule.

Quantum chemical calculations

In order to confirm the interpretation of the NMR results, conformational analysis was performed on compounds **1**, **4**, **6**, and **7** with the use of quantum chemical (PM3) calculations. Conformations were investigated by rotating the phenolic, dibromophenolic and α-naphtholic rings for compounds **1**, **4**, and **6**, respectively, in steps of 20°.

At each step, complete geometry optimization was performed. The results are reported in Table 3. For each conformation, as defined by the value of the dihedral angles ϑ_1 (ring 1) and ϑ_2 (ring 2), we report the energy relative to the global minimum and the angles $\hat{A}_1$ and $\hat{A}_2$ that rings 1 and 2 form with the phthalidic ring. The averaged angle ($\hat{A}_{avg}$) is also reported, since shielding/deshielding effects over the phthalidic ring come from both rings 1 and 2.

Inspection of the ΔE values in Table 3 shows that phenolphtalein (**1**) has very low rotational barriers (less than 1 kcal/mol). The rotational profile is drawn in Figure 6a. Two minima occur at 300 and 340°. Since the rotation of the phenolic ring has a periodicity of 180°, these minima are equivalent to the 120 and 160° in Figure 6a. The dibromo analogue (**4**) possesses a very similar rotational profile to that of phenolphthalein (Table 3). As regards the α-naphtolic analogue (**6**), the rotational profile is not 180° periodic and, as expected, is characterized by high rotational barriers between conformers. Three clear minima are detected at 300, 200, and 80°, plus a shallow minimum at 340° (Fig. 6b). Finally, the rigid analogue **7** assumes a conformation were $\vartheta_1 = 55.5°$ and $\vartheta_2 = 124.1°$: the geometries of compounds **1**, **6**, and **7** are drawn in Figure 7.

Angles $\hat{A}_1$ and $\hat{A}_2$ reported in Table 3 are suitable indicators of conformation to account for the observed trend of H4 chemical shifts in our series. Compound **7** is blocked in a nearly perpendicular conformation having $\hat{A}_1 = 92.5°$ and $\hat{A}_2 = 92.7°$ ($\hat{A}_{avg} = 92.6°$). This is consistent with the lowest H4 chemical shift observed for this compound because H4 falls inside the shielding cones of the two rings. Phenolphthalein (**1**), the dibromo analogue (**7**) and the naphthyl analogue (**6**) have $\hat{A}_{avg}$ values higher than 90°, which indicates a deshielding effect of rings 1 and 2 over the common phthalidic ring. Interestingly, $\hat{A}_{avg}$ values of the dibromo analogue are always higher than the corresponding values for phenolphthalein (Table 3), in agreement with the higher H4 chemical shift of compound **4** with respect to that of **1**. Even more significant is that the $\hat{A}_{avg}$ values of compound **6** are substantially lower than those of **1** and **4**, again in accord with the lower chemical shift of H4 in compound **6**. The $\hat{A}_{avg}$ descriptor of conformation thus succesfully accounts for the observed trend of H4 chemical shift in our series; the closer to perpendicularity the $\hat{A}_{avg}$ values, the lower the H4 chemical shift. It is particularly interesting that this is found for every value of ϑ_1, the chemical shift being related more to a medium effect over the NMR time scale than to a single minimum energy conformation. Only two exceptions occur at $\vartheta_1 = 240$ and 260° where compound **6** has $\hat{A}_{avg}$ values slightly higher than **1**; however, these are unstable conformations in which the naphthyl ring is significantly distorted and the computation of $\hat{A}_1$ and $\hat{A}_2$ suffers the highest deviation from the mean value (see computational details).

One way to obtain a single descriptor of conformation for each compound is to weight the $\hat{A}_{avg}$ values with the energy associated with that particular conformation; in fact, values of $\hat{A}_{avg}$ corresponding to energy minima contribute more than values associated with high energy conformations to the overall chemical shift result. The weighting factor was calculated from the ΔE values in Table 3 using the Boltzmann equation, and then normalized to give a total of 1 over the 0–360° conformational scan. For the blocked compound **7**, the weighted $\hat{A}_{avg}$ coincides with the original value (92.6°); for compounds **1**, **4**, and **6** values of 118.2, 119.3, and 113.0° were obtained, respectively; these values correlated very well with the H4 chemical shifts and reinforced the link between calculated angles and H4 chemical shifts.

One interesting result is that the lowest energy conformation of **6** ($\vartheta_1 = 300°$) fully agrees with the conformation inferred from NMR data at low temperature (see Fig. 8 in the Conclusion).

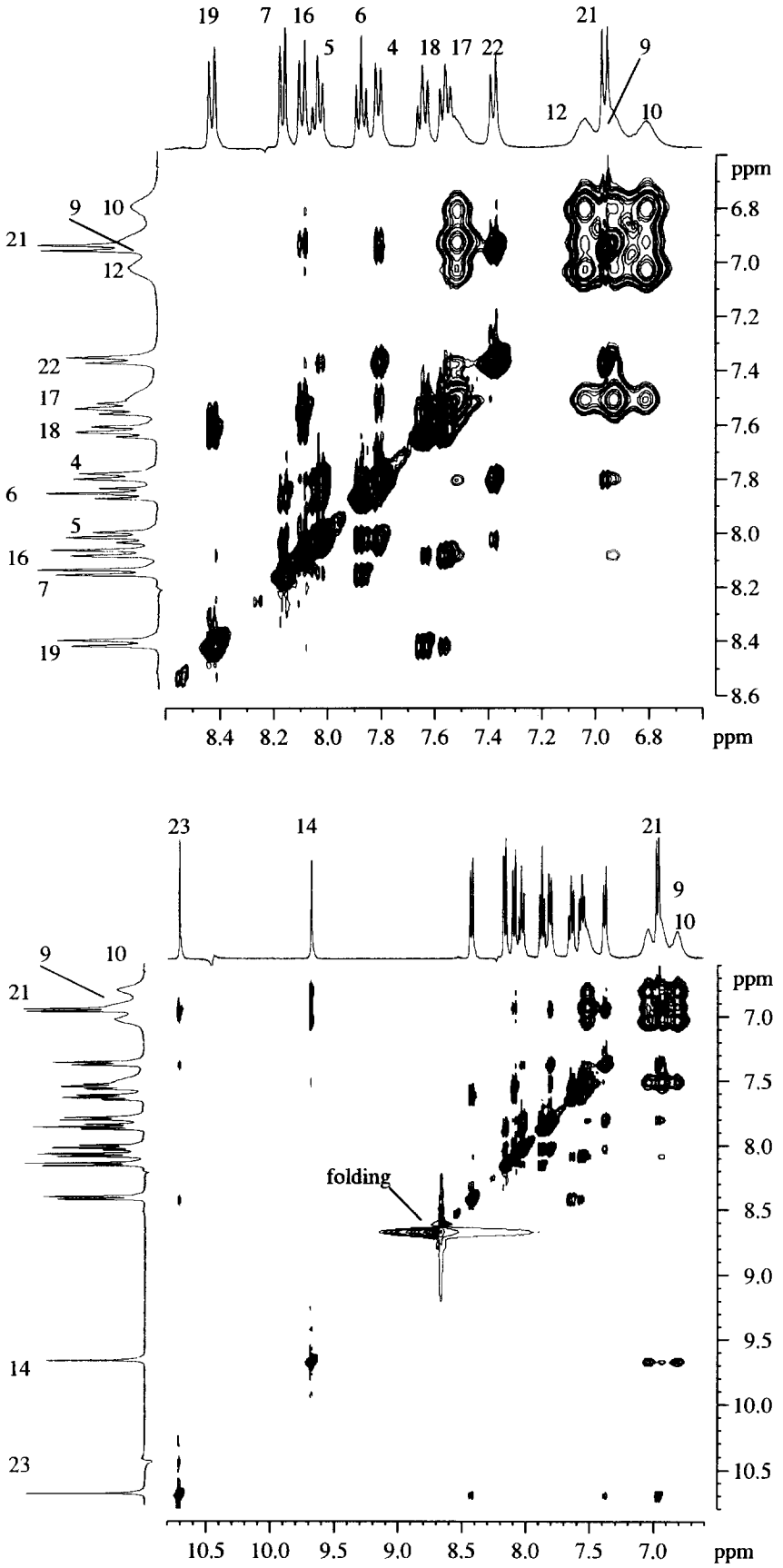

Figure 5. ^{1}H/2-D NOESY spectrum of compound **6** recorded at 179 K in acetone-d_6 using 600 ms of mixing time.

Table 3. Conformational analysis results for compounds **1**, **4**, and **6**[a]

Compound **1**						Compound **4**					Compound **6**				
ϑ_1[b]	ϑ_2[b]	ΔE[c]	$\hat{A}_1$[d]	$\hat{A}_2$[d]	$\hat{A}_{avg}$[e]	ϑ_2	ΔE	$\hat{A}_1$	$\hat{A}_2$	$\hat{A}_{avg}$	ϑ_2	ΔE	$\hat{A}_1$	$\hat{A}_2$	$\hat{A}_{avg}$
0	−163.9	0.55	118.5	124.4	121.5	−164.6	0.49	118.5	124.5	121.5	−117.5	1.28	118.6	114.7	116.7
20	−146.9	0.67	107.9	126.9	117.4	−148.1	0.65	108.1	127.1	117.6	−124.0	2.26	107.2	113.3	110.3
40	−153.5	0.84	98.6	125.6	112.1	−154.1	0.89	98.7	125.7	112.2	−130.2	3.14	102.2	112.8	107.5
60	−164.7	0.77	90.2	123.3	106.8	−163.9	0.88	90.1	123.7	106.9	−143.0	2.91	92.2	113.0	102.6
80	−170.6	0.47	98.8	121.8	110.3	−169.3	0.58	98.9	122.5	110.7	−170.0	2.54	102.8	114.6	108.7
100	−172.4	0.19	108.3	122.3	115.3	−171.0	0.24	108.4	123.0	115.7	−172.3	3.87	112.2	114.6	113.4
120	−172.7	0.14	116.9	123.6	120.3	−171.3	0.11	117.0	124.4	120.7	163.4	5.09	120.8	105.9	113.4
140	−172.8	0.56	122.8	124.9	123.9	−171.6	0.43	122.9	125.6	124.3	159.0	6.49	111.3	106.1	108.7
160	−158.4	0.36	126.4	126.9	126.7	−159.0	0.16	126.5	127.0	126.8	−99.9	4.50	103.4	114.7	109.1
180	−163.1	0.72	120.6	124.5	122.6	−163.9	0.64	120.6	124.6	122.6	−107.0	0.95	111.2	112.9	112.1
200	−147.1	0.81	107.5	126.9	117.2	−148.4	0.74	107.9	127.1	117.5	−108.1	0.52	117.3	110.4	113.9
220	−154.2	0.93	98.1	125.5	111.8	−154.7	0.93	98.4	125.6	112.0	−115.6	3.25	110.4	109.8	110.1
240	−164.2	0.81	90.0	123.4	106.7	−163.5	0.88	90.0	123.7	106.9	−164.9	5.54	102.0	115.9	109.0
260	−170.1	0.48	98.3	121.9	110.1	−168.9	0.57	98.5	122.5	110.5	−176.5	3.42	109.3	113.0	111.2
280	−172.4	0.12	107.7	122.0	114.9	−171.0	0.19	107.9	122.8	115.4	178.7	1.27	115.1	112.6	113.9
300	−173.0	0	116.4	123.4	119.9	−171.3	0	116.6	124.2	120.4	163.6	0	114.3	107.0	110.7
320	−173.0	0.42	122.2	124.8	123.5	−171.7	0.35	122.5	125.5	124.0	167.4	1.35	129.8	110.2	120.0
340	−156.9	0.19	125.7	127.2	126.5	−157.5	0.05	126.0	127.2	126.6	−110.9	1.15	125.5	114.9	120.2

[a]Compound **7**, the rigid analogue in our series, has the following conformation: $\vartheta_1 = 55.5°$, $\vartheta_2 = 124.1°$, $\hat{A}_1 = 92.5°$, $\hat{A}_2 = 92.7°$, $A_{avg} = 92.6ß$.
[b]Dihedral angles for the rotations of rings 1 (ϑ_1) and 2 (ϑ_2).
[c]Relative energies (kcal/mol) of each conformation with respect to the global minimum.
[d]Angles (°) that rings 1 ($\hat{A}_1$) and 2 ($\hat{A}_2$) form with the phthalidic ring.
[e]The averaged value of $\hat{A}_1$ and $\hat{A}_2$.

Finally, there is a qualitative agreement between the conformation of phenolphthalein (**1**) bound to TS in the crystal structure of the inhibitor–enzyme complex and the conformation here calculated. Ring 1 binds TS with $\vartheta_1 = 292°$, very close to the calculated global minimum energy conformation ($\vartheta_1 = 300°$); ring 2 is rotated about 40°. However, the remarkable conformational freedom of the phenyl ring demostrated by both NMR and quantum chemical calculations allows the optimal steric fit of phenolphthalein into the binding site of the enzyme at very little cost in energy.

Structure–activity analysis

We synthesized compounds **2** and **3** (chloro derivatives of phenolphthalein) to complete the series of the halogeno derivatives of this class of compounds and compound **6**, as previously described.[6–8] The apparent inhibition constants (K_{iapp} values) of LcTS for the compounds under investigation are reported in Table 4.

It is reasonable to suppose that all the compounds bind in a similar position of the active site, because they are structurally analogous and all have the same inhibition pattern.[4,5] It is also resonable from a structural point of view since the *ortho* subsituents on the phenolic rings can be easily accommodated in the binding site pocket, and the phenolic rings have considerable conformational freedom around the C3–C8 and C3–C15 bonds.

Compounds **1**, **2**, **4**, and **5** can be regarded as a unique group having very similar inhibitory properties ranging from 1 to 5 μM K_{iapp}. Compound **3** is slightly less active (11 μM). Compound **6** is still active despite the introduction of the bulky naphthyl ring; inspection of the X-ray structure of the binary complex TS-phenolphthalein shows that **6** could be fitted rigidly into the binding pocket with a conformation corresponding to that of the calculated lowest energy conformation. The slightly lower activity, compared with that of **1–5**, is more likely to be due to the reduced conformational freedom observed in this molecule.

Fluorescein (**7**) should be regarded more carefully: rigid matching of **7** with the X-ray crystal structure of the binary complex TS–phenolphthalein indicates that the two phenolic rings, which have rigid conformations, assume different orientations with respect to **1**. However, this rotation does not seem so important as to account for the complete loss of activity of fluorescein. An explanation may be that the pK_a of fluorescein are very low compared with those of phenolphtalein.[16,17] Since at pH 7.4 the molecule is completely dissociated and the lactonic ring is in the open form, the species interacting with the enzyme is completely different from the neutral one. This could explain the high IC_{50} value (600 μM). We cannot measure the intrinsic binding capability of the neutral form of fluorescein in the standard buffer because it is not present at pH 7.4.

Conclusion

In the present work we have characterized the structures of some phthalein derivatives through ^1H NMR and quantum chemical calculations with complete geometry optimization. The data analysis suggests a good agreement between the NMR results and the

theoretical calculations. In particular: (a) the chemical shift of the H4 proton is a good indicator of the average conformations that the phenolic rings assume with respect to the phthalidic ring. About molecules **7**, **6**, **1**, **4**, the closer to perpendicularity the $\hat{A}_{avg_2}$ values the lower the H4 chemical shift. The lower the $\hat{A}_{avg_2}$, the higher the intensity of the shielding effect of the phenolic rings on the H4 proton; (b) the chemical shifts of the protons of the phenolic rings in structures **1–5** and that of the α-naphthol ring in structure **6** are very similar to the chemical shift of the corresponding protons of the non-linked fragments **8–10**. This observation suggests that the aromatic rings are free to rotate around bonds C3–C8 and C3–C15 independently of the dimension of the halogen in the *ortho* position. In fact, had there been conformational constraints, the resonance frequencies would have been shifted considerably in structures **1–6** with respect to structures **8–10**. A further finding supporting the conformational freedom is that the NOEs H4-H9, H16 and H4-H13, H20 in structure **2** have the same intensity as those observed in structure **6** between H4 and H16 and between H4 and H22. These findings are also in agreement with the calculated conformational profile shown in Figure 6a, where very low conformational barriers are detected that show that there are no preferred conformations; and (c) the conformational freedom of compound **1** is still present at low temperature (179 K), where the resonance frequencies of H13 and H20 protons are still indistinguishable from those of H9 and H16 protons. Compound **6** maintains rotational freedom up to 250 K; at 240 K, the H9 and H13 protons begin to differentiate and at 220 K, H10 also begin differentiating from H12. At 179 K, H9, H13 and H10, H12 are completely different. This indicates that, at 179 K, a preferred confomation exists for the phenolic ring of **6**. The two-dimensional NOESY spectrum confirms this finding and shows unambiguously that the preferred conformation from NMR coincides with the lowest energy conformation here calculated (Fig. 8).

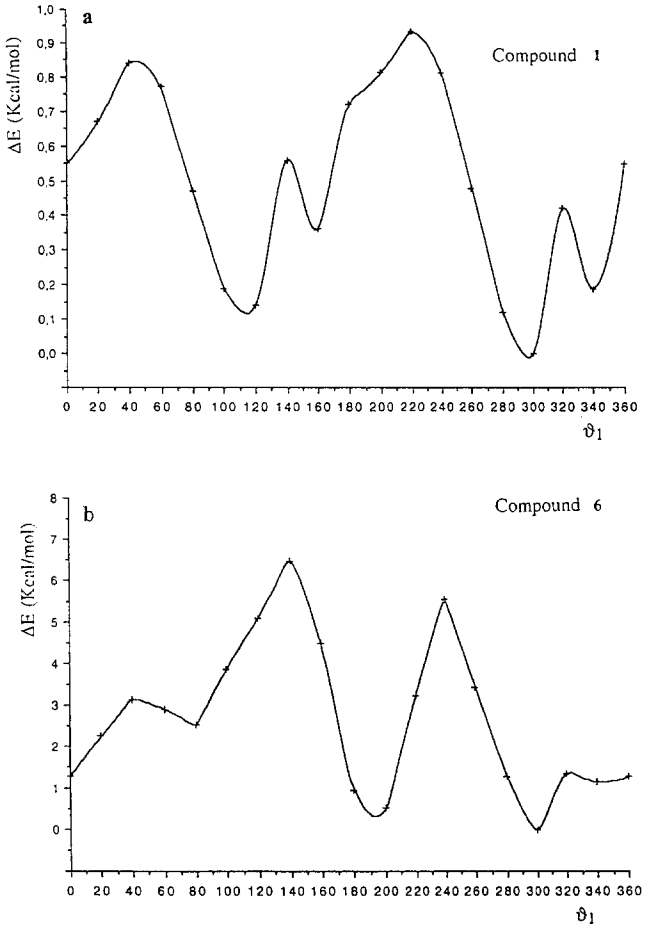

Figure 6. Rotational profile for compounds **1** (a) and **6** (b). The solid line is obtained from interpolation of the calculation results every 20° as described in the Experimental section.

A qualitative relationship between the conformations of the molecules and their inhibitory properties can be

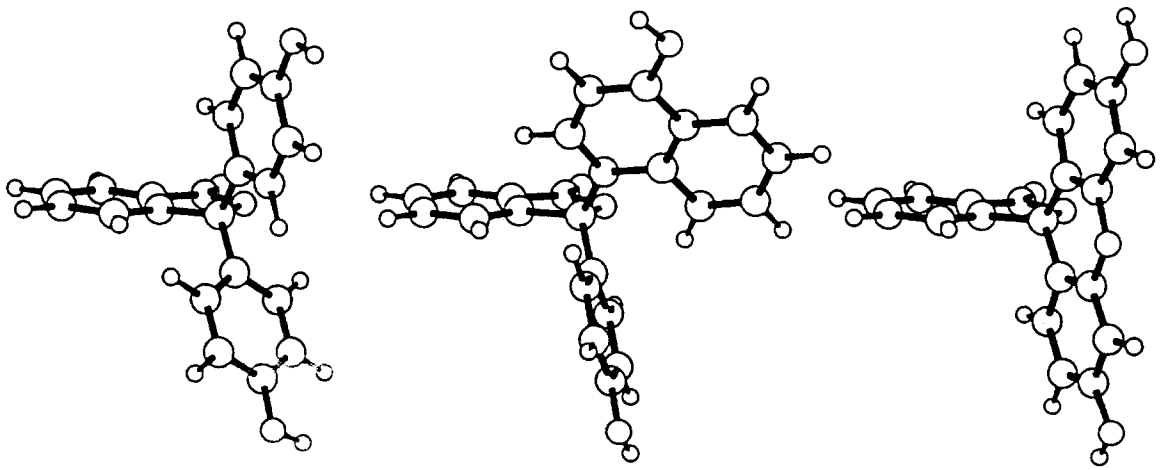

Figure 7. More stable conformations for compounds **1** and **6**, and that of the rigid analogue **7**. The differences in $\hat{A}_1$ and $\hat{A}_2$ angles for the compounds can be observed.

Table 4. Apparent K_i (K_{iapp}) and IC_{50} for the compounds studied[a]

Compound	K_{iapp}	IC_{50}
1	4.7	—
2	1.7	—
3	11.0	—
4	3.4	—
5	0.9	—
6	20.0	—
7	—	600

[a]The standard errors from nonlinear least-squares fit of the experimental data are less than 20% for all values.

observed: molecules with high rotational freedom at the phenolic ring (**1–5**) are more active than that with a partially blocked conformation (**6**). This could be due to the enhanced ability of the compound to adapt its conformation to the binding pocket. Other factors can contribute to the inhibitory properties of the molecules, such as the proton donor capability of the oxydrilic group, but the NMR chemical shifts of the oxydrilic protons are not so different in the series **1–7** (Table 1) and they do not match with biological activity trend.

We can conclude that ^{1}H NMR and quantum chemical data afford valuable insight into the conformational behaviour of phthaleins and suggests some of the structural requirements necessary to maintain a good initial inhibitory activity in the phthalein series, such as a non-rigid analogue, conformational freedom of the aromatic substituents at the quaternary carbon, a phenolic ring with at least one *ortho* substituent, and no interference by the proton donor capability (polarization) of the phenolic hydroxyl group.

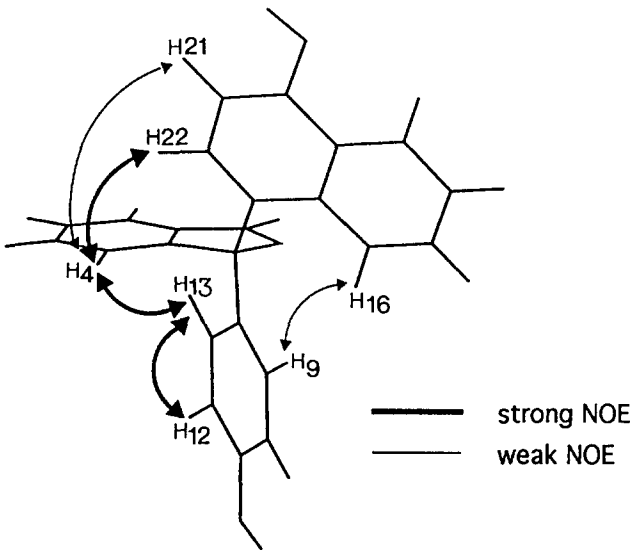

Figure 8. Compound **4** is reported with the conformation supported by ^{1}H/2-D NOESY spectrum at 179 K in acetone-d_6 (see Figs 4 and 5). The protons showing NOEs are indicated by arrows. Calculated interatomic distance are as follow: 2.46 Å (H4–H13), 4.63 Å (H4–H21), 2.55 Å (H4–H22), 2.76 Å (H9–H16), 2.49 Å (H12–H13).

Experimental

Chemistry

The compounds have been prepared with modifications of known methods.[8–10] Melting points were determined on a Buchi 510 capillary melting points apparatus and are uncorrected. Analyses indicated by the symbols were within ±0.4 of the theoretical values. TLC on silica gel plates was used to check product purity. Silica gel 60 (Merck; 70–230 mesh) was used for column chromatography. The structures of all the compounds were consistent with their analytical and spectroscopic data. Compounds **1**, **4**, **5**, and **7** were purchased from Sigma.

[bis-3′-Chloro-4′-hydroxyphenyl]-3-phthalide (2). A mixture of phthalide (2 g, 0.0135 mol), *o*-chlorophenol (3.02 g, 0.027 mol) and a few drops of sulfuric acid was heated at 180–190 °C for 5 h. After cooling, the residue was dissolved in dichloromethane and purified by silica gel chromatography, eluting with cyclohexane:ethyl acetate (60:40). Yield 80%, mp 88–90 °C. Anal. $C_{20}H_{12}Cl_2O_4$ (C, H, Cl).

[bis-3′,5′-Dichloro-4′-hydroxyphenyl]-3-phthalide (3). Compound **3** was prepared in the same way as **2**, starting from phthalide and 2,6-dichlorophenol. Yield 3%, mp 210 °C. Anal. $C_{20}H_{10}Cl_4O_4$ (C, H, Cl).

[4′-Hydroxyphenyl-4′-hydroxynaphtyl]-3-phthalide (6). A mixture of 2(4′-hydroxybenzoyl)benzoic acid (2 g, 0.0082 mol) and thionyl chloride (5 mL) was refluxed for 8 h. After cooling, the excess thionyl chloride was evapd under vacuum, the residue was dissolved in toluene (5 mL) and a solution of α-naphthol (1.19 g, 0.0082 mol) was added dropwise. After stirring for 2 h at 40 °C, the mixture was cooled and the resultant precipitate was filtered under vacuum and purified by silica gel chromatography, eluting with cyclohexane:ethyl acetate (70:30). Yield 23%, mp 255–258 °C. Anal. $C_{24}H_{16}O_4$ (C, H).

NMR spectra

All NMR measurements were performed at the frequency of protons on a Bruker AMX 400 WB spectrometer operating at 9.395 Tesla. Spectra were performed on 16 mM compound dissolved in DMSO-d_6 for analysis at 303 K, or in acetone-d_6 for studies at 179 K.

2-D COSY[11] spectra were recorded using 512 or 1024 time-domain points and 128 or 256 increments (F_1 dimension), depending on the spectral width employed, 1 s of relaxation delay and 8 transients per increment. Data were doubled in F_1 dimension by zero filling and weighted by a sine-bell functions in both dimensions before Fourier transformation. This last was run in magnitude mode.

2-D NOESY[12] spectra were acquired with TPPI Phase Cycle,[13] $256(F_1) \times 1024(F_2)$ or $512(F_1) \times 1024(F_2)$ data points, depending on the spectral width used, 1 s of relaxation delay, 8 scans per transient and using mixing times of 200 ms and 600 ms. Data were weighted before Fourier transformation using sine square-bell function shifted of $\pi/2$ radiants in both dimensions.

Selective 1-D COSY spectra[14] were acquired using selective 80 ms Gaussian shaped pulse truncated at 1% of the maximum amplitude.

Quantum chemical calculations

Conformational analysis was performed on compounds **1**, **4**, **6**, and **7** using the MOPAC[15] program in the PM3 parameterization.[14] Since the di-halogen substituted phenolphthaleins have very similar proton H4 chemical shift values, calculations were performed on one only namely, the di-bromo compound **4**, which has the highest H4 chemical shift value.The rotational profiles were obtained by rotating the phenolic (**1**), dibromophenolic (**4**) and the α-naptholic (**6**) rings in steps of 20°. Once the dihedral angle that controls the rotation (91) had been set, all the other geometric parameters were optimized using very tight gradient (GNORM = 0.0001) and convergence (SCFCRT = 1.0 D-10) criteria. For the rigid analogue **7**, only one complete geometry optimization was necessary to determine its conformation.

The angles that rings 1 ($\hat{A}_1$) and 2 ($\hat{A}_2$) form with the phtalidic ring were taken as indicators of conformation pertinent to the comparison with the NMR data (Fig. 9). $\hat{A}_1$ and $\hat{A}_2$ were computed using the cartesian coordinates of three nonconsecutive atoms on ring 1, three on ring 2, and three on the phthalidic ring for each conformation. More than one selection of three atoms was performed in order to average differences arising out of slight distorsions of the rings, especially for the most hindered high-energy conformations. All calculations were performed on a Convex C220 computer at the Centro Interdipartimentale di Calcolo ed Elettronica Applicata (CICAIA) of the University of Modena.

Enzyme assay

Lactobacillus casei TS was purified to electrophoretic homogeneity following a known procedure.[17] The activity of the enzyme was determined spectrophotometrically by standard TS assay following increasing absorbance at 340 nm due to the formation of 7,8-dihydrofolate, as reported.[18]

Assays were performed in standard TES buffer which contained 50 mM TES pH 7.4, 4.25 mM $MgCl_2$, 6.5 mM formaldehyde, 1 mM EDTA and 75 mM 2-mercapto-ethanol. The concentrations of dUMP, CH_2H_4 folate, and enzyme were 120, 140, and 0.07 μM, respectively.

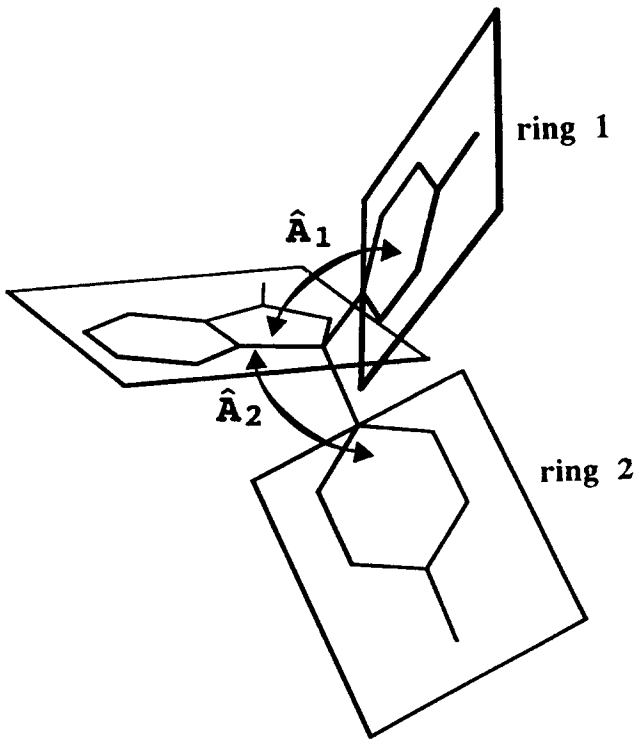

Figure 9. Angles that ring 1 ($\hat{A}_1$)and 2 ($\hat{A}_2$) form with the plane of the phthalidic ring in phenolphthalein (**1**).

Inhibitory activity was determined by steady-state kinetic experiments, followed by classical Lineweaver–Burk plot analysis: the effect on TS activity of various substrate concentrations in the presence of different inhibitor concentrations was studied (**1** and **6**).[17a] The reaction mixture consisted of standard TES buffer, dUMP 120 μM, 6,l-(*R*,*S*)-folate 5–140 μM ($0.5–8 \times K_m$) and inhibitor 0.001–100 μM. For compound **7** only the IC_{50} value was obtained: the inhibitory property of the compound was determined by measuring the effect of six different inhibitor concentrations on the standard mixture formed by dUMP 120 μM and l-(*R*,*S*)-folate 82 μM. The same experimental conditions were kept to determine the apparent K_i (K_{iapp}) for the other compounds (**2**, **3**, **4**, and **5**). K_i values were obtained by nonlinear least-square fit of the residual TS activity as a function of inhibitor concentration to the suitable equations for competitive inhibition[19b] using the Kaleidagraph program (Abelbeck Software, Reading, PA 1989) on a Macintosh computer.

Acknowledgements

We thank CIGS (Centro Interdipartimentale Grandi Strumenti) dell'Università di Modena for supplying NMR spectrometer CICAIA (Centro Interdipartimentale di Calcolo Elettronico) for computing facilities, Dr Brian Shoichet for the X-ray crystal structure of the LcTS–phenolphthalein complex, Mrs Soragni Fabrizia for her excellent technical assistance and Professor Toma Luciano for the critical reading of the manuscript.

References

1. Santi, D. V.; Danenberg, P. V. In *Folate and Pteridines*; Blakeley R. L.; Benkovic S. J., Eds.; Wiley: New York, 1984; pp 345–398.

2. Douglas, K. T. *Med. Res.* **1987**, *7*, 441.

3. Shoichet, B. K.; Perry, K. M.; Stroud, R. M.; Santi, D. V.; Kuntz, I. D. *Science* **1993**, *259*, 1445.

4. Costi, M. P.; Pecorari, P.; Rinaldi, M.; Barlocco, D.; Shoichet, K. B.; Kuntz, I. .D.; Santi, D. V.; Stroud, R M. XII Symposium on Medicinal Chemistry, 19–23 September 1993, Parigi Abstr. P44.

5. Costi, M. P., personal comunication.

6. Sjoback, J.; Nygren, J.; Kubista, M. *Spectros. Acta Part A* **1995**, *51*, L7.

7. Ozeki, T.; Morikawa, H.; Kihara, H. *Comp. Aided Innoovation New Material II* **1993**, 925.

8. Haubacher, M. *J. Am. Chem. Soc.* **1944**, *66*, 255.

9. Blicke, F. F.; Patelski, R. A. *J. Am. Chem. Soc.* **1938**, *69*, 2283.

10. Blicke, F. F.; Swisher, R. D. *J. Am. Chem. Soc* **1934**, *56*, 902.

11. Aue, W. P.; Batholdi, E.; Ernst, R. R. *J. Chem. Phys.* **1976**, *64*, 2229.

12. Jeener, J.; Meier B. H.; Bachmann P.; Ernst R. R. *J. Chem. Phys.* **1979**, *71*, 4546.

13. (a) Redfield, A. G.; Kunz, S. D. *J. Magn. Res.* **1975**, *19*, 250. (b) Bodenhausen, G.; Vold, R. L.; Vold, R. R. *J. Magn. Res.* **1980**, *37*, 93.

14. Bauer, C.; Freeman, R.; Frenkiel, T.; Keeler, J.; Shanka *J. Magn. Res.* **1984**, *58*, 442.

15. Stewart, J. J. P. MOPAC 6.0, QCPE 455.

16. Stewart, J. J. P. *J. Comp. Chem.* **1989**, *10*, 209.

17. Climie, S. C.; Santi, D. V. *Proc. Natl. Acad. Sci. U.S.A* . **1990**, *87*, 633.

18. Pogolotti, A. L.; Danenberg, P. U.; Santi, D. V. *J. Med. Chem.* **1986**, *29*, 478.

19. (a) Segel, I. H. *Enzyme Kinetics*; Wiley: New York, 1975; p 172. (b) *ibidem*, p 109.

(*Received in U.S.A.* 29 *April* 1996; *accepted* 16 *July* 1996)